

PAPER • OPEN ACCESS

A Comparison of Soil Structure Interaction Models for Dynamic Analysis of Offshore Wind Turbines

To cite this article: Breiffni Fitzgerald *et al* 2020 *J. Phys.: Conf. Ser.* **1618** 052043

View the [article online](#) for updates and enhancements.



IOP | ebooks™

Bringing together innovative digital publishing with leading authors from the global scientific community.

Start exploring the collection—download the first chapter of every title for free.

A Comparison of Soil Structure Interaction Models for Dynamic Analysis of Offshore Wind Turbines

Breiffni Fitzgerald, David Igoe and Saptarshi Sarkar

Department of Civil, Structural and Environmental Engineering, School of Engineering,
Trinity College Dublin, Ireland.

E-mail: breiffni.fitzgerald@tcd.ie

Abstract. This paper compares the dynamic response of an OWT structure where the below ground pile-soil behaviour is modelled using (i) the conventional API ‘p-y’ approach and (ii) the ‘PISA’ approach. A nonlinear aero-elastic code is used to model the structural dynamics of the OWT and coupled to the geotechnical model. The dynamic behaviour (natural frequencies) and fatigue loads of the turbine tower and monopile are estimated and compared using both the API and PISA approaches. A limited number of load cases were considered in the dynamic analysis with varied met-ocean conditions. It was found that the stiffer springs estimated by the PISA approach reduce the mean displacement of the tower in both the fore-aft and side-to-side directions. However, the increased monopile stiffness leads to a slightly increased amplitude of oscillations, particularly in the lightly damped side-to-side direction.

1. Introduction

Monopiles are the most widely used foundation support system for offshore wind turbines (OWTs). More than 80% of recent offshore wind turbine installations in Europe rely on monopile support structures. The design length of a monopile is typically governed by lateral loading requirements related to serviceability, displacement and rotation limits. The monopile diameter is often governed by dynamic lateral and rotational stiffness requirements as part of the OWT natural frequency and structural fatigue checks. The standard industry approach for the geotechnical design of monopiles in Europe is as recommended by Det Norske Veritas - Germanischer Lloyd (DNV-GL) [1], which is based on American Petroleum Institute (API) design guidelines [2]. The API guidelines were originally developed and intended for the design of offshore oil and gas jacket piles. The API method uses a decoupled Winkler beam approach [3] where the lateral soil reaction is described by non-linear p-y springs. The API methods were calibrated using a limited number of pile tests performed on slender jacket piles with diameters less than 1 m and are now recognized as being unsuitable for predicting the response of large diameter monopiles. Recent advances in monopile design approaches [4, 5, 6] have allowed for significant optimization of the foundation design and fatigue life of the structure, resulting in large cost savings for OWTs supported on monopiles. The new monopile geotechnical design approach, termed the ‘PISA’ design model is an outcome of the UK Carbon Trust PISA research project that included field testing at two onshore sites and three-dimensional (3D) finite element modelling, and represents the current state-of-the-art in monopile geotechnical design. Similar to the API approach, the new PISA design model is implemented in a generalised form of



the Winkler framework, where the soil reactions (forces and moments) are related to the pile displacements and rotations.

This paper compares the dynamic response of an OWT structure where the below ground pile-soil behaviour is modelled using:

- (i) the conventional API p-y approach, and
- (ii) the new PISA design model approach.

The new PISA design model includes a number of different soil reaction components in addition to the lateral soil reaction, p , such as distributed moments, m , due to the vertical tractions on the pile as well as base shear, H_B , and base moment, M_B components, as shown in Figure 1. The PISA design model has developed a new set of calibrated non-linear curves for each soil reaction component, which are applied in a one-dimensional (1D) finite element model. The difference in stiffness between the two approaches is compared and the outputs were used in separate dynamic wind turbine models to assess the effect on the overall structure's fundamental natural frequency and the fatigue life of the tower.

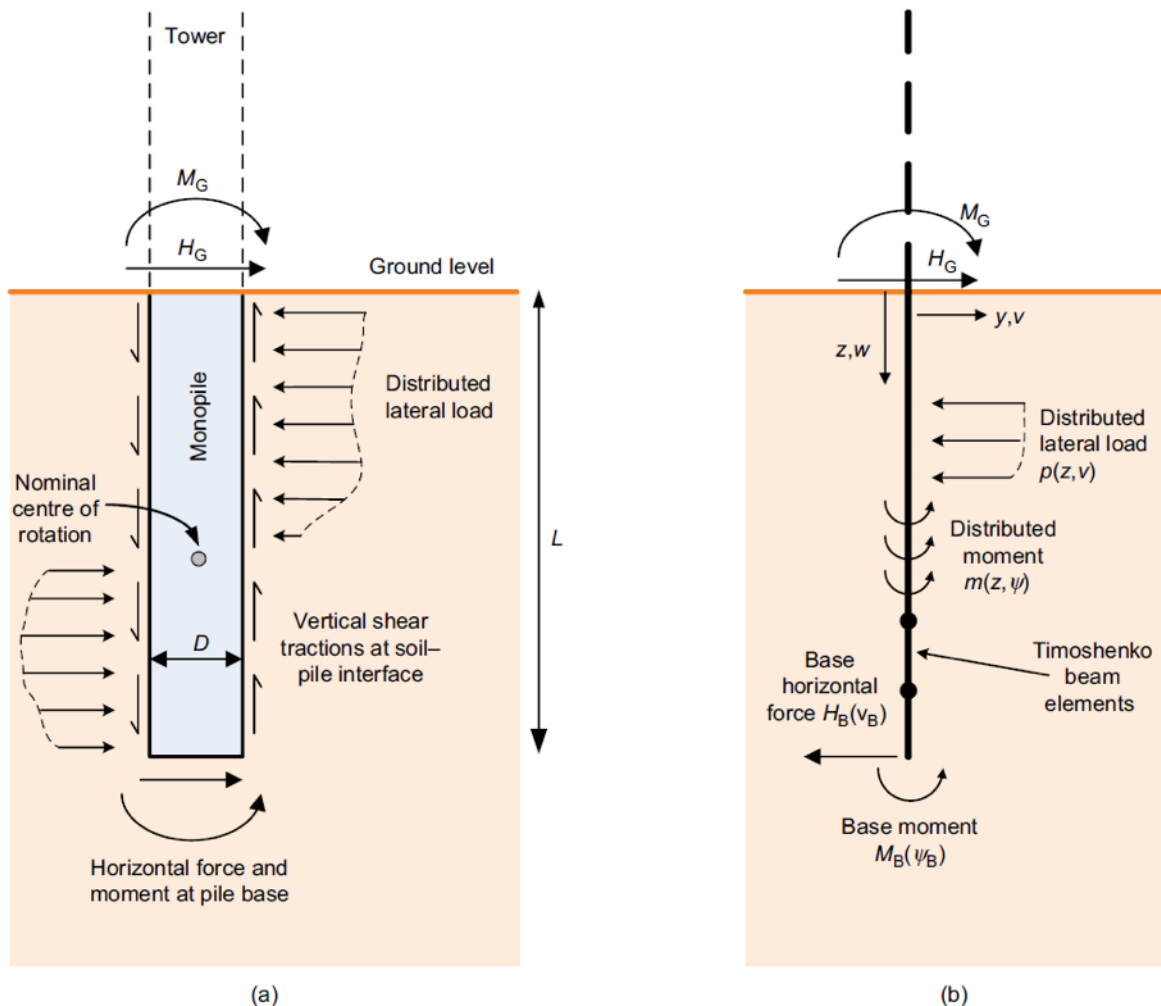


Figure 1. PISA design model: (a) idealisation of the soil reaction components acting on the pile; (b) 1D finite-element implementation of the model showing the soil reactions acting on the pile, after [6]

A multibody dynamic model of an offshore wind turbine is developed using Kane's method, this model has previously been benchmarked against the United States National Renewable Energy Laboratory's (NREL) FAST model [7, 8]. Blade element momentum theory and Morison's equation are used to estimate the turbulent aerodynamic and hydrodynamic loads respectively. The structural model is coupled to the geotechnical model and the dynamic behaviour (natural frequencies) and fatigue loads of the turbine tower and monopile are estimated and compared using both the API and PISA approaches.

2. Methodology

2.1. Geotechnical modelling

For the purposes of this paper, the soil was modelled as a stiff clay with properties deemed representative of stiff clay deposits in the North Sea. The primary soil inputs in cohesive soils (clays) for the API and PISA soil reaction curves are the soil saturated unit weight, γ_{sat} , clay undrained shear strength, c_u , a strain parameter ϵ_c (determined from undrained triaxial compression laboratory tests) and the small strain modulus of the soil, G_0 . The soil input parameters were estimated based on experience and details are provided in Table 1.

γ_{sat}	20 [kN/m ³]
c_u	80 + 4z [kPa]
ϵ_c	0.005
G_0	1000 p'_0 [kPa]

Table 1. Soil parameter details

Where z is the depth below mudline and p'_0 is the mean effective stress at a given depth. For the purposes of modelling the below mudline pile response, an initial approximate monopile geometry for the site was determined using the API method to ensure it passes serviceability (SLS) checks, such that the permanent rotation at mudline is limited to $< 0.25^\circ$, and Ultimate Limit State (ULS) checks, such that the maximum rotation at mudline under factored extreme loads are $< 1.5^\circ$. Approximate loads were used for the geotechnical analysis whereby an SLS horizontal load $H_{SLS} = 8000$ kN was assumed to act at an eccentricity (height above mudline) of 30 m. The ULS load $H_{ULS} = 10800$ kN was assumed by factoring the H_{SLS} by 1.35. These loads were used to approximately size the monopiles. Based on the API approach this resulted in a pile which was 8 m in diameter, 28 m embedment with a constant 60 mm wall thickness below mudline. It should be noted that using the new PISA design model, it is possible to design a pile with significantly smaller dimensions, as shown by [9] and others. However for the purpose of comparing the dynamic response of the OWT structure using the two different geotechnical approaches, the geometry is kept the same.

In order to apply a linearized foundation stiffness in the dynamic wind turbine structural model, the operational stiffness of the monopile was determined using an equivalent fatigue horizontal load, H_{FLS} , of 2000 kN, which was deemed to be representative of typical operational loads. The equivalent linearized stiffness was then determined for each spring under the H_{FLS} applied load using both the API and PISA approaches and the outputted deflections and rotations are shown in Figure 2. It is clear that the PISA design model results in a pile response which is significantly stiffer than the API approach, resulting in a mudline deflection which is approximately half of that determined using the API method. The resulting soil reaction linearized secant stiffnesses were then applied in the structural model as described in the following section.

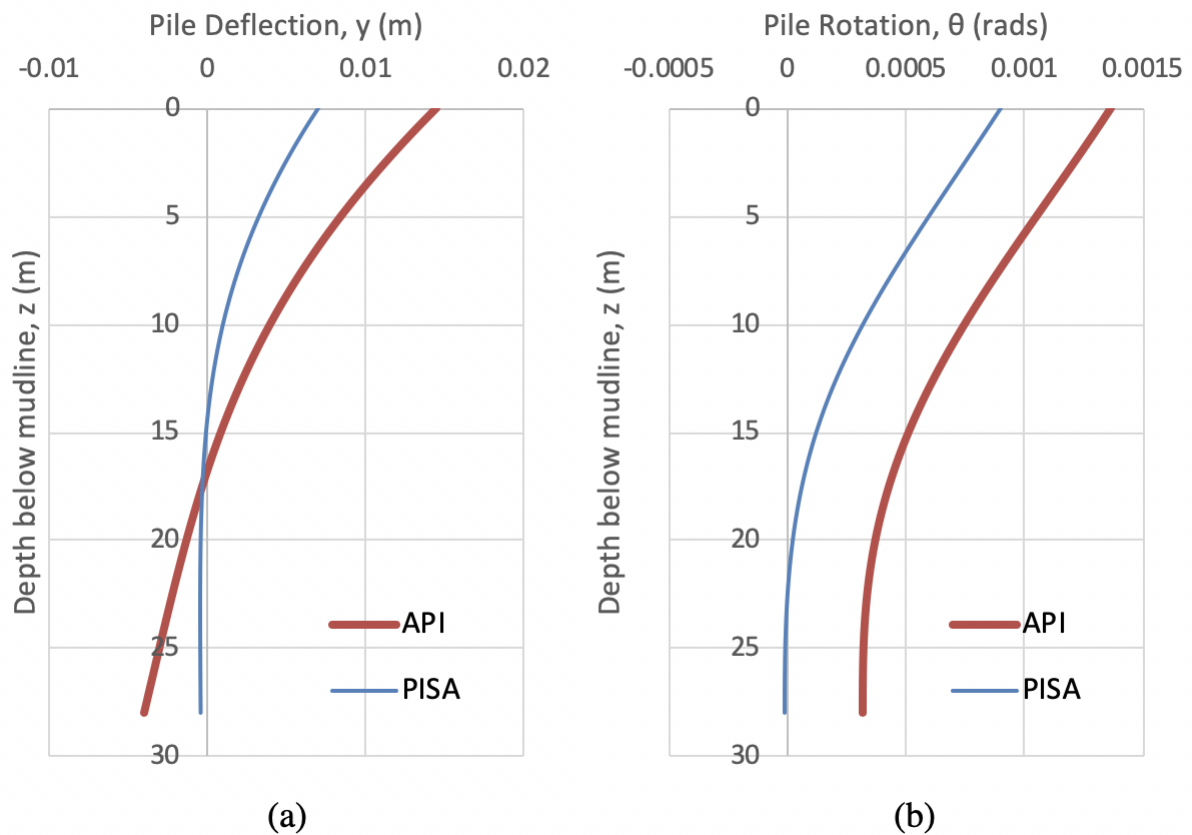


Figure 2. Pile (a) deflection and (b) rotation response under equivalent operation load $H_{FLS} = 2000$ kN

2.2. Structural modelling

A nonlinear aero-elastic code developed by Sarkar et al. [7, 8] that implements a blade element momentum (BEM) technique to model the aerodynamics, Morison's equation to model the hydrodynamic loads and mode shapes for the structural dynamic modelling is used for dynamic analysis of the OWT. The nonlinear aero-elastic model of the wind turbine is derived using Kane's equation [10] and is written in MATLAB. It has 22 degrees of freedom and is numerically benchmarked against FAST [11].

When modelling a multi-body system like a offshore wind turbine, it is necessary that every component is defined in its local coordinate system and then referred back to the global, in this case, inertial reference frame denoted by \hat{z} . Figure 3 illustrates the different reference frames. Local coordinate systems are assigned to the tower base (\hat{a}), tower nodes, tower-top (\hat{b}), nacelle (\hat{d}), low-speed shaft (\hat{e}), azimuth (\hat{e}) and the blades (\hat{g}). The blades have more than one coordinate system assigned to them. For detailed modelling of the blades, they are referred to their coned coordinate system (\hat{i}) followed by the pitched coordinate system (not pictured). Aerodynamic loads are applied on the blade nodes that are not only coned and pitched but also rotated due to elastic deformation of the blades in out-of-plane and in-plane directions. The coordinate systems used (except the tower and blade element fixed coordinate systems and blade pitched coordinate system) are shown in Figure 3.

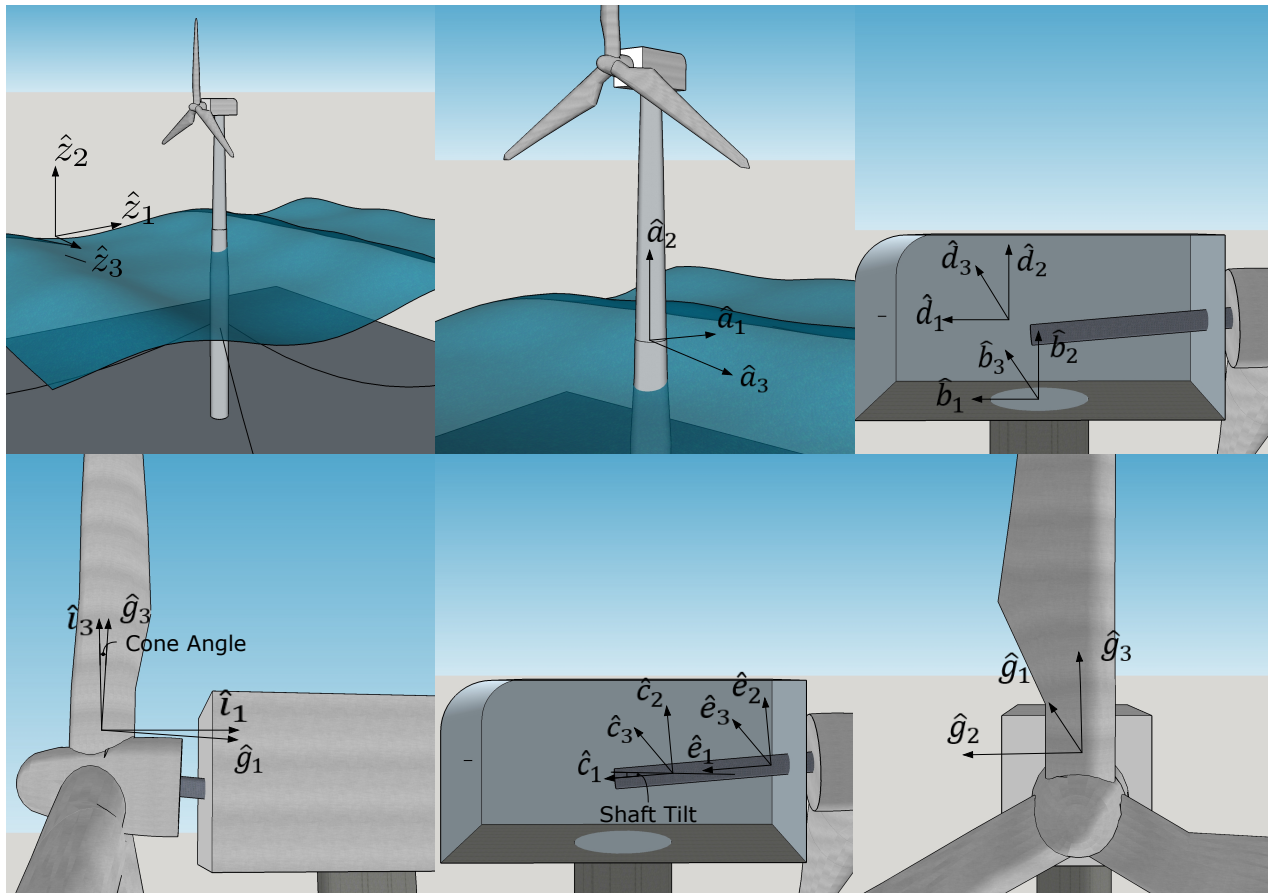


Figure 3. Coordinate systems defined in structural model

Kane’s equations of motion for a simple holonomic multi-body system can be stated as [10]

$$F_k + F_k^* = 0 \quad \text{for } k = 1, 2, \dots, N \quad (1)$$

where, N is the total number of degrees of freedom required to describe the complete kinematics of the wind turbine system. With a set of M rigid bodies characterized by reference frame N_i and center of mass point X_i , the *generalized active force* associated with the k^{th} degree of freedom is given as [10]

$$F_k = \sum_{i=1}^M \left[{}^E \mathbf{v}_k^{X_i} \cdot \mathbf{F}^{X_i} + {}^E \omega_k^{N_i} \cdot \mathbf{M}^{N_i} \right] \quad (2)$$

where \mathbf{F}^{X_i} is force vector acting on the center of mass of point X_i and \mathbf{M}^{N_i} is the moment vector acting on the N_i rigid body. ${}^E \mathbf{v}_k^{X_i}$ and ${}^E \omega_k^{N_i}$ are the partial linear and partial angular velocity of the point X_i and rigid body N_i respectively associated with the k^{th} degree of freedom in the inertial (E) reference frame. The *generalized inertia force* for k^{th} degree of freedom is given as

$$F_k^* = - \sum_{i=1}^M \left[{}^E \mathbf{v}_k^{X_i} \cdot (m^{N_i} {}^E \mathbf{a}^{X_i}) + {}^E \omega_k^{N_i} \cdot {}^E \dot{\mathbf{H}}^{N_i} \right] \quad (3)$$

where it is assumed that for each rigid body N_i , the inertia forces are applied at the centre of

the mass point X_i . ${}^E\dot{\mathbf{H}}^{N_i}$ is the time derivative of the angular momentum of rigid body N_i about its center of mass X_i in the inertial frame [10].

For the wind turbine model, the mass of the tower, yaw bearing, nacelle, hub, blades, generator contributes to the total generalized inertia forces. Generalized active forces are the forces applied directly to the wind turbine system, forces that ensure constraint relationships between the various rigid bodies and internal forces within flexible members. Forces applied directly on the offshore wind turbine system include aerodynamic forces on the blades and the tower, hydrodynamic forces on the monopile, gravitational forces, generator torque, high-speed shaft brake. In this work gearbox friction forces have been neglected. Yaw springs and damper contribute to forces that enforce constraint relationship between rigid bodies. Internal forces within flexible members include elasticity and damping in tower, blades and drive-train. For further details on the aero-elastic structural model please refer to several previous works by the authors [7, 8, 12, 13].

The structural model includes distributed lateral and rotational springs below the mudline to represent the soil-monopile. The foundation is modelled using Winkler springs for the soil. The tower-monopile assembly is considered as a single flexible member with varying sectional properties. The tower-monopile assembly along with the Winkler springs are modelled in the finite element code BModes [14] distributed by NREL to extract its modal properties. The first two mode shapes in the fore-aft direction and the side-to-side direction are used in the dynamic analysis. The finite element analysis is performed separately for different distributed spring constants obtained from the API and PISA method. This leads to different mode shapes and fundamental frequencies for the two different foundation models, see Table 2.

API		PISA	
Fore-Aft	Side-to-Side	Fore-Aft	Side-to-Side
0.243	0.242	0.251	0.249

Table 2. Natural frequencies obtained from finite element analysis using BModes (in Hz)

3. Numerical simulations

Numerical simulations are performed under a stochastic wind-wave loading scenario. Eleven load cases are studied in the paper. Different turbulent wind fields with varying hub-height wind speeds are generated using TurbSim [15]. The turbulence intensity in the wind is assumed to be 10%. The stochastic sea is modelled using the Pierson-Moskowitz spectrum [16] with varying wave heights and wave periods. Cases with wind wave misalignments are also considered where the wave is incident on the turbine at an angle relative to the wind. The different load cases and the environmental conditions are summarised in Table 3. All simulations are executed for the standard duration of 10 minutes and the initial 50 seconds of the response is removed to account for transience. Table 4 summarises the mudline bending moments in the fore-aft and side-to-side directions for the different load cases estimated for the two different methods of modelling the soil. It can be observed that in all cases the PISA method estimates a stiffer pile and hence the DELs are higher compared to the API method. And lastly, Table 5 presents the average DELs of the 11 load cases analysed in this paper and their corresponding percentage increase using the PISA method. It is important to note here that these values are simply arithmetic average of the different load cases and are not weighted by their probability of occurrence. The authors are currently working on this to estimate the lifetime increase of mudline bending moment DELs that results from the use of the PISA method to model the pile foundation.

Time domain simulations of the mudline bending moment in the fore-aft and side-to-side directions for load case 7 are shown for illustration in Figures 4 and 5 respectively.

Load Case (#)	Rotor speed (RPM)	Wind Speed (m/s)	Wave height (m)	Wave direction (deg)	Wave period (sec)
1	11.2	8	1	0	6
2	12.1	11.4	1	0	6
3	12.1	13	1	0	6
4	12.1	13	2	30	6
5	12.1	15	2	0	6
6	12.1	15	2	60	6
7	12.1	17	3	0	6
8	12.1	17	2	90	6
9	12.1	19	4	0	7
10	12.1	21	4	45	8
11	12.1	23	6	0	8

Table 3. Load cases considered

Load Case (#)	Fore Aft		Side to Side	
	API	PISA	API	PISA
1	2.61E+003	2.76E+003	1.17E+003	1.37E+003
2	3.95E+003	3.98E+003	1.66E+003	2.31E+003
3	4.86E+003	4.85E+003	2.46E+003	3.12E+003
4	5.53E+003	5.81E+003	4.85E+003	6.49E+003
5	5.15E+003	5.54E+003	1.50E+003	1.70E+003
6	4.28E+003	4.40E+003	8.56E+003	1.48E+004
7	6.09E+003	6.91E+003	1.84E+003	2.47E+003
8	3.99E+003	3.93E+003	1.05E+004	1.77E+004
9	6.79E+003	7.51E+003	3.96E+003	3.74E+003
10	6.10E+003	6.41E+003	6.51E+003	1.19E+004
11	9.00E+003	9.68E+003	6.15E+003	6.19E+003

Table 4. Mudline Bending Moment DELs (kNm)

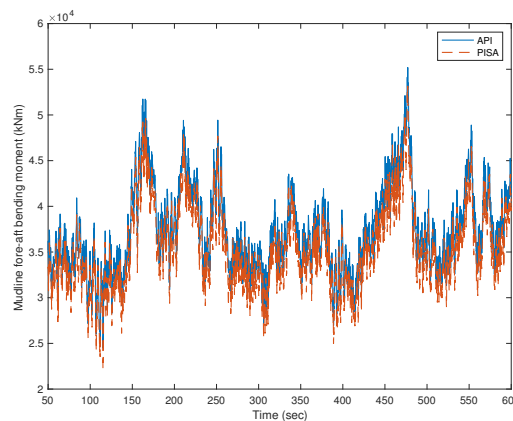


Figure 4. Mudline bending moment in fore-aft direction

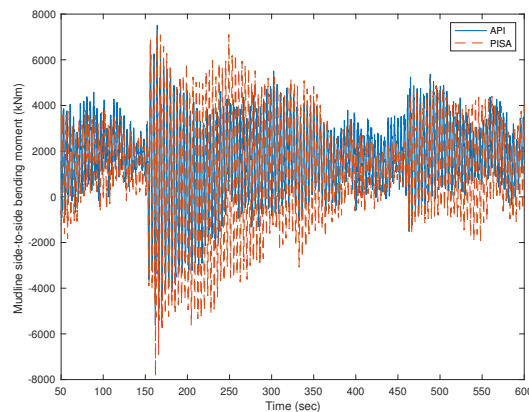


Figure 5. Mudline bending moment in side-to-side direction

The PISA method estimates stiffer springs, this leads to reduced mean tower displacement in both the fore-aft and side-to-side directions when compared to the API method. However, the increase in monopile stiffness with no associated damping increase leads to slightly amplified amplitude of vibrations, especially in the tower side-to-side mode which experiences very little aerodynamic damping. This behaviour is clearly seen in Figures 4 and 5.

3.1. Effects on fatigue life

Fatigue Damage Equivalent Loads (DELs) of the tower mudline bending moment in the fore-aft and side-to-side case are calculated. The DELs are estimated using the classical rainflow counting technique [17]. The DELs are obtained as the constant amplitude loads of fixed amplitude and a frequency of 1 Hz. The first 50 seconds of the time history load predictions are removed from the analysis to remove starting transient effects as is standard in dynamic analysis of wind turbines [18, 19]. Table 5 presents the mudline bending moment DELs calculated from the API and PISA approaches averaged over all load cases considered. Since the DEL depends more on the amplitude of oscillation than the mean response, the estimated DELs from the PISA method are slightly higher than those obtained by the API method. This is especially the case for the tower side-to-side mode. There is approximately a 46% increase in the fatigue DELs in the side-to-side mode. This is due the increased amplitude of tower vibrations and low aerodynamic damping in this direction. The misaligned wind-wave loads also contributed to this averaged figure. A more modest increase of 6% is shown in the higher damped fore-aft direction.

Fore-Aft			Side-to-Side		
API	PISA	% increase	API	PISA	% increase
5.30E+003	5.62E+003	6%	4.47E+003	6.53E+003	46%

Table 5. Average mudline bending moment DEL (kNm)

4. Conclusions

This paper compared the dynamic response of an OWT structure where the below ground pile-soil behaviour was modelled using (i) the conventional API ‘p-y’ approach and (ii) the ‘PISA’ approach. The difference in stiffness estimated by the two approaches was compared and the outputs were used in separate dynamic wind turbine models to assess the effect on the dynamics of the structure and the fatigue life of the tower. The structural model was

coupled to the geotechnical model and the dynamic behaviour (natural frequencies) and fatigue loads of the turbine tower and monopile were estimated and compared using both the API and PISA approaches. A limited number of load cases were considered in the dynamic analysis with varied met-ocean conditions. It was found that the stiffer springs estimated by the PISA approach reduce the mean displacement of the tower in both the fore-aft and side-to-side directions. However, the increased monopile stiffness leads to a slightly increased amplitude of oscillations, particularly in the lightly damped side-to-side direction. The increased oscillation leads to increased DELs. Therefore, from this initial study it appears that the API method may underestimate the tower fatigue DELs in the side-to-side direction. It should be noted that a limited number of load cases have been examined and soil damping also has not been considered. Future studies must address these two limitations of the study. In addition to this, it is important that a future study validates the new modelling approach with measured data since the ‘ground truth’ should be established when comparing one model with another.

5. Acknowledgments

The support of the Sustainable Energy Authority of Ireland (Grant No. RDD/213 & Grant No. RDD/511) is appreciated.

References

- [1] DNV G 2016 *DNVGL-ST-0126: Support structures for wind turbines*
- [2] API 2000 Recommended practice for planning, designing and constructing fixed offshore platforms—working stress design— Tech. rep. American Petroleum Institute
- [3] Winkler E 1867 *Theory of elasticity and strength* (Prague: Dominicus)
- [4] Zdravković L, Jardine R J, Taborda D M, Abadias D, Burd H J, Byrne B W, Gavin K G, Houlsby G T, Igoe D J, Liu T *et al.* 2019 *Géotechnique* 1–16 ISSN 0016-8505
- [5] Burd H J, Taborda D M, Zdravković L, Abadie C N, Byrne B W, Houlsby G T, Gavin K G, Igoe D J, Jardine R J, Martin C M *et al.* 2019 *Géotechnique* 1–50 ISSN 0016-8505
- [6] Byrne B W, Houlsby G T, Burd H J, Gavin K G, Igoe D J, Jardine R J, Martin C M, McAdam R A, Potts D M, Taborda D M *et al.* 2020 *Géotechnique* 1–18 ISSN 0016-8505
- [7] Sarkar S and Fitzgerald B 2020 *Structural Control and Health Monitoring* **27** e2471
- [8] Sarkar S, Chen L, Fitzgerald B and Basu B 2020 *Journal of Sound and Vibration* **470** 115170 ISSN 0022-460X
- [9] Doherty P, Jalilvand S, Lapastoure L M and Igoe D 2020 *International Symposium for Frontiers in Offshore Geotechnics (ISFOG2020)*
- [10] Kane T R and Levinson D A 1985 *Dynamics, theory and applications* (McGraw Hill)
- [11] Jonkman J M and Buhl M 2005 *FAST Users Guide* (NREL/EL-500-38230 (previously NREL/EL-500-29798), Golden, CO: National Renewable Energy Laboratory)
- [12] Igoe D, Prendergast L J, Fitzgerald B and Sarkar S 2018 *Proceedings of China-Europe Conference on Geotechnical Engineering* (Springer) pp 340–343
- [13] Sarkar S, Fitzgerald B and Basu B 2020 *IEEE Transactions on Control Systems Technology*
- [14] Bir G 2005 User’s guide to bmodes (software for computing rotating beam-coupled modes) Tech. rep. National Renewable Energy Lab.(NREL), Golden, CO (United States)
- [15] Jonkman B J and Buhl Jr M L 2006 Turbsim user’s guide Tech. rep. National Renewable Energy Lab.(NREL), Golden, CO (United States)
- [16] Pierson Jr W J and Moskowitz L 1964 *Journal of geophysical research* **69** 5181–5190
- [17] Downing S D and Socie D 1982 *International journal of fatigue* **4** 31–40
- [18] Fitzgerald B and Basu B 2017 *Struct. Monit. Maint* **4** 175–194
- [19] Fitzgerald B, Staino A and Basu B 2019 *Structural Control and Health Monitoring* **26** e2284